



ISSN No. : 2321-9653

IJRASET

**International Journal for Research in Applied
Science & Engineering Technology**

IJRASET is indexed with Crossref for DOI-DOI : 10.22214

Website : www.ijraset.com, E-mail : ijraset@gmail.com

Certificate

*It is here by certified that the paper ID : IJRASET25903, entitled
Pyrrolone Antimalarials: Pharmacophoric Analysis using In-Silico
Techniques*

by

Atul V. Ingle

*after review is found suitable and has been published in
Volume 7, Issue XII, December 2019*

in

*International Journal for Research in Applied Science &
Engineering Technology*

Good luck for your future endeavors

By [Signature]

Editor in Chief, IJRASET



ISRA Journal Impact
Factor: **7.429**



45.98
INDEX COPERNICUS



THOMSON REUTERS
Researcher ID: 115581-2016



TOGETHER WE REACH THE GOAL
SJIF 7.429

PRINCIPAL

Yeshwantrao Chavan College of
Arts, Commerce & Science, Sillod
Dist. Aurangabad.





Pyrrolone Antimalarials: Pharmacophoric Analysis using In-Silico Techniques

Nilesh S. Kadu¹, Atul V. Ingle²¹Department of Chemistry, Bharatiya Mahavidyalaya, Amravati, Maharashtra, India²Department of Chemistry, Yeshwantrao Chavan College of Arts, Commerce and Science, Sillod, Tq. Sillod, Dist. Aurangabad, Maharashtra, India

Abstract: In the present work, extensive pharmacophore modelling has been completed to recognize the consensus and significant structural features having relationship with antimalarial activity of Pyrrolone derivatives. The selected dataset encompasses of sixty-one Pyrrolone derivatives showing the anti-plasmodial activity (EC_{50}) against Pfk1 strain in the range 0.07 to 33.73 μ M. For consensus modelling, out of sixty-one, the five utmost active molecules were aligned using common structural features, followed by pharmacophore modelling using PyMOL. The consensus pharmacophore model identified some vital structural features which could be used in future optimizations of these congeneric molecules.

Keywords: Pharmacophore modelling, antimalarial activity, Pyrrolone derivatives, Drug design

I. INTRODUCTION

Malaria is a vector borne (Mosquito) deadly parasitic disease with significant presence in undeveloped and developing countries from Africa and Asia. The disease is instigated by parasites of the *Plasmodium* genus, generally by *Plasmodium falciparum*, and accountable for more than 214 million cases in 2015. World Health Organization (WHO) endorses artemisinin combination therapies (ACT) for treatment of malaria. But recent reports indicate the appearance of resistance against ACT, particularly from Southeast Asia [1-4]. Consequently, developing a novel drug for malaria is a necessity. Unfortunately, designing a new drug using conventional methodologies is a hard, 10-15 years long, expensive and often associated with high risks of let-down. Hence, alternate approaches like Computer Aided Drug Design (CADD) should be used with high importance.

CADD is a method of choice due to many advantages like result oriented performance, cheaper, less time and resource consumption, and provides alternative to animal testing. CADD has gained this reputation due to its thriving branches like pharmacophore modelling, QSAR, etc. The technique of pharmacophore modelling provides key features to be retained in future optimizations for drug development [5-7]. Hence, in this analysis, we have developed consensus pharmacophore model for antimalarial activity of Pyrrolone derivatives. Recently, Murugesan *et al* [3] reported antimalarial activity of Pyrrolone derivatives. The newly synthesized molecules were tested for anti-plasmodial activity (EC_{50}) which varies in the range 0.07 to 33.73 μ M. Though, SAR (Structure Activity Relationship) were discussed by them, but no attempt was executed to create consensus pharmacophore model. This is first ever attempt to derive consensus pharmacophore model for antimalarial activity of Pyrrolone derivatives using a simple approach. The results could be beneficial to medicinal chemists while developing new drugs for malaria using Pyrrolone derivatives as the starting material.

II. EXPERIMENTAL METHODOLOGY

1) **Dataset:** The dataset consists of sixty-one Pyrrolone derivatives exhibiting the anti-plasmodial activity (EC_{50}) in μ M range. The Pyrrolone derivatives possess good variation in substitution pattern like the presence of different heterocyclic, aliphatic and aromatic rings, positional isomers and change in linkers [1]. Therefore, the selected dataset is wide enough to develop a consensus pharmacophore model. The dataset has been tabulated in table 1. For the sake of comparison, the EC_{50} have been transformed to p EC_{50} .

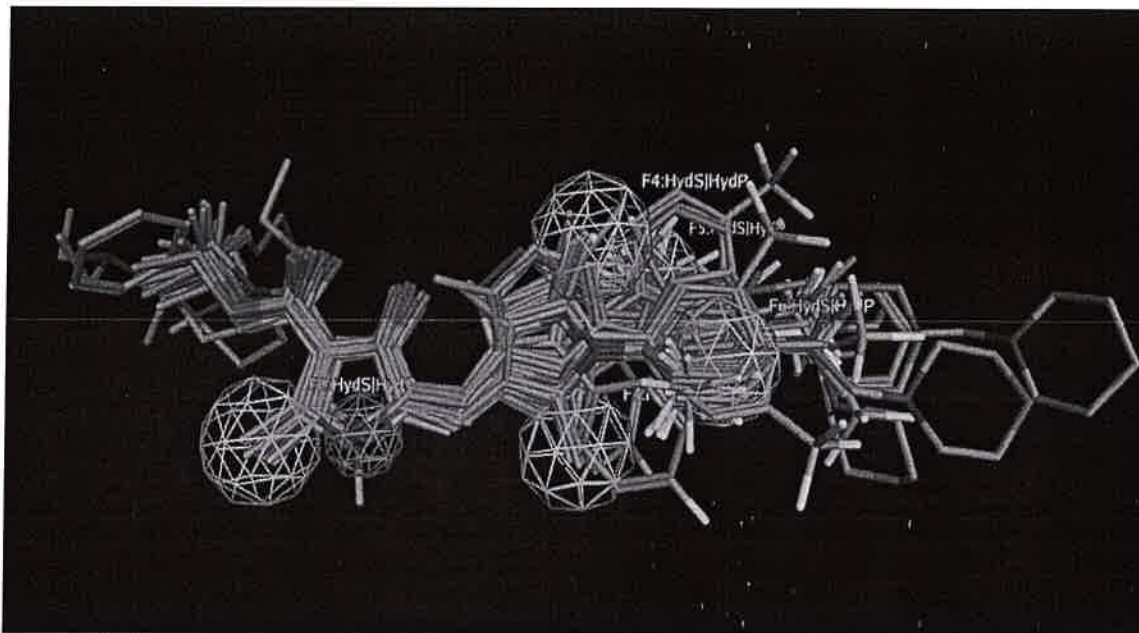
Table 1. Five most active Pyrrolone derivatives (SMILES notation) along with reported p EC_{50} used in the present work

S.N.	SMILES notation	p EC_{50}
1.	<chem>O=C(OC)C=1C(=O)/C(NC=1C)=C\c3cc(n(c2c(ccc2)C(F)(F)F)c3C)</chem>	8.155
2.	<chem>O=C(OCC)C=1C(=O)/C(NC=1C)=C\c3cc(C)n(c2ccc(SC(F)(F)F)cc2)</chem>	8.097
3.	<chem>O=C(OCC)C=1C(=O)/C(NC=1C)=C\c3cc(C)n(c2ccccc2C(F)(F)F)c3C</chem>	8.046
4.	<chem>O=C(OCC)C=1C(=O)/C(NC=1C)=C\c3cc(C)n(c2ccc(cc2)C(F)(F)F)</chem>	7.721
5.	<chem>O=C(OCC)C=1C(=O)/C(NC=1C)=C\c3cc(n(c2c(ccc2)C(F)(F)F)c3CC)</chem>	7.699

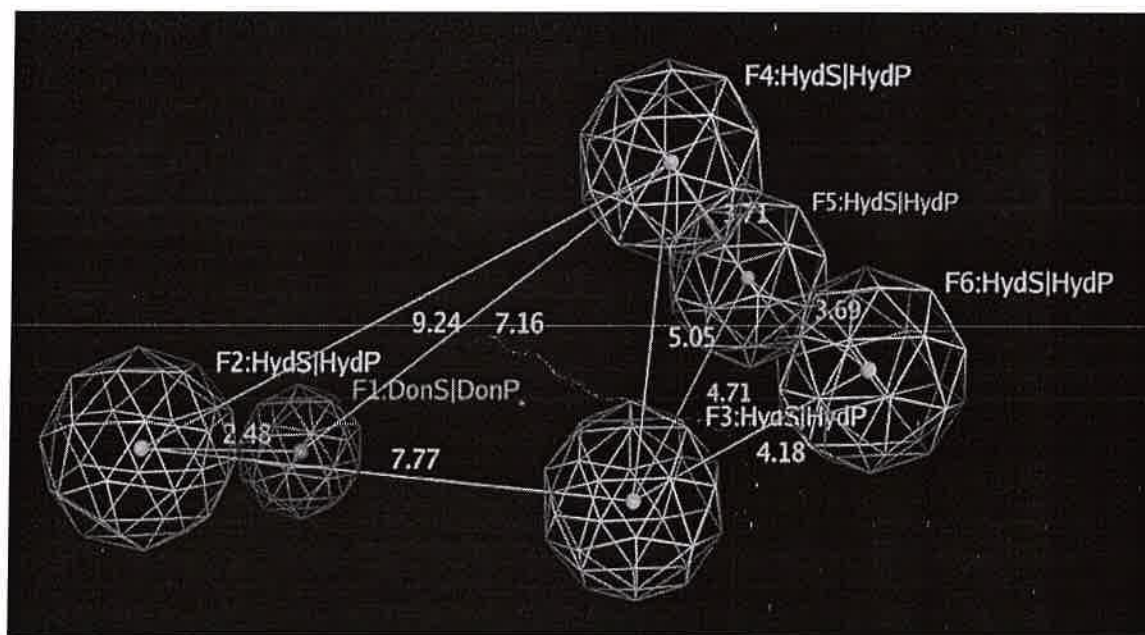


- 2) *Structure Drawing, Optimization and Alignment [5-7]:* The standard procedure for developing consensus pharmacophore modelling [5-7] has been followed. The four main steps are:
- Step-1:* The structures were drawn using ChemSketch 2010 freeware
 - Step-2:* Optimization using PM3 semi-empirical method using MOPAC 2012
 - Step-3:* Alignment of molecules using Open3dAlign software
 - Step-4:* Using the default settings, consensus pharmacophore model was created using PyMOI 1.8.6

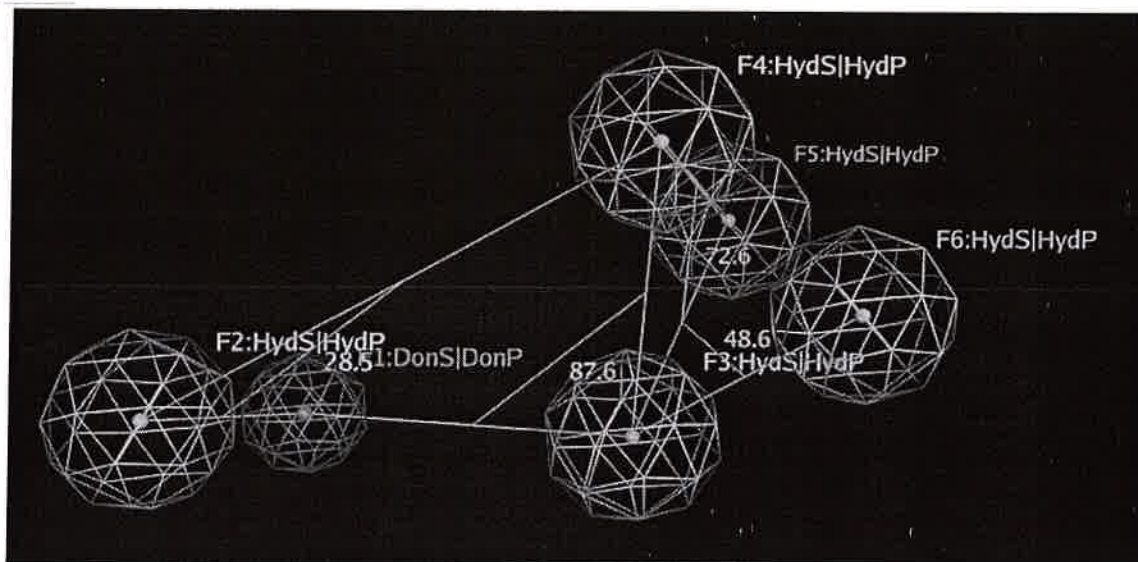
III. RESULTS AND DISCUSSION



(a)



(b)



(c)

Figure 1. 3D- representation of consensus pharmacophoric pattern using all molecules (Yellow: Hydrophobic, Green: H-Bond donor regions) (a) All molecules with pharmacophore model (b) Distances between pharmacophoric regions (c) Angles between pharmacophoric regions

The consensus pharmacophore modelling identified six important regions in the molecules which have correlation with anti-malarial activity of Pyrrolone derivatives. The most prominent regions are: (1) five hydrophobic regions (shown by yellow contours), (2) A H-bond donor region (shown by green contour). These regions are spread across the molecules with three aromatic/hydrophobic regions in the close proximity of each other. In future optimizations these regions should be retained for good activity.

IV. CONCLUSIONS

The present work revealed important pharmacophoric patterns for anti-malarial activity of Pyrrolone derivatives.

REFERENCES

- [1] Singh, K., Okombo, J., Brunschwig, C., Ndubi, F., Bamard, L., Wilkinson, C., . . . Chibale, K. (2017). Antimalarial Pyrrolone derivatives: Lead Optimization, Parasite Life Cycle Stage Profile, Mechanistic Evaluation, Killing Kinetics, and in Vivo Oral Efficacy in a Mouse Model. *Journal of Medicinal Chemistry*, 60(4), 1432-1448
- [2] World Health Organization (WHO). World Malaria Report 2015. http://www.who.int/malaria/publications/world_malaria_report_2015/wmr-2015-no-profiles.pdf?ua=1; Geneva, Switzerland
- [3] Murugesan, D., Mital, A., Kaiser, M., Shackleford, D. M., Morizzi, J., Katneni, K., . . . Gilbert, I. H. (2013). Discovery and Structure–Activity Relationships of Pyrrolone Antimalarials. *Journal of Medicinal Chemistry*, 56(7), 2975-2990.
- [4] Dondorp, A. M.; Nosten, F.; Yi, P.; Das, D.; Phyto, A. P.; Tarning, J.; Lwin, K. M.; Arley, F.; Hanpithakpong, W.; Lee, S. J.; Ringwald, P.; Silamut, K.; Imwong, M.; Chotivanich, K.; Lim, P.; Herdman, T.; An, S. S.; Yeung, S.; Singhasivanon, P.; Day, N. P.; Lindergardh, N.; Socheat, D.; White, N. J. Artemisinin Resistance in *Plasmodium falciparum* Malaria. *N. England Journal of Medicine*. 2009, 361, 455-467.
- [5] Masand, V. H., & Rastija, V. (2017). PyDescriptor : A new PyMOL plugin for calculating thousands of easily understandable molecular descriptors. *Chemometrics and Intelligent Laboratory Systems*, 169, 12-18.
- [6] Masand, V. H., El-Sayed, N. N. E., Mahajan, D. T., & Rastija, V. (2017). QSAR analysis for 6-arylpyrazine-2-carboxamides as *Trypanosoma brucei* inhibitors. *SAR and QSAR in Environmental Research*, 28(2), 165-177.
- [7] Masand, V. H., El-Sayed, N. N. E., Mahajan, D. T., Meherdar, A. G., Alkafay, A. M., & Shibi, I. G. (2017). QSAR modeling for anti human African trypanosomiasis activity of substituted 2-Phenylimidazopyridines. *Journal of Molecular Structure*, 1130, 711-718.






ISSN No. : 2321-9653

IJRASET

**International Journal for Research in Applied
Science & Engineering Technology**

IJRASET is indexed with Crossref for DOI-DOI : 10.22214

Website : www.ijraset.com, E-mail : ijraset@gmail.com

Certificate

*It is here by certified that the paper ID : IJRASET25621, entitled
Study of Structural, Optical & Solid State Properties of Nanocrystalline
Cadmium Sulfide Thin Films*

by

A. V. Ingle

*after review is found suitable and has been published in
Volume 7, Issue XI, November 2019*

in

*International Journal for Research in Applied Science &
Engineering Technology*

Good luck for your future endeavors

Py

Editor in Chief, IJRASET

[Signature]

PRINCIPAL

**Yeshwantrao Chavan College of
Arts, Commerce & Science, Sils:
Dist. Aurangabad**



ISRA
JIF

ISRA Journal Impact
Factor: 7.429



45.98
INDEX COPERNICUS



THOMSON REUTERS
Researcher ID: N-9631-2016



TOGETHER WE REACH THE GOAL
SJIF 7.429



Study of Structural, Optical & Solid State Properties of Nanocrystalline Cadmium Sulfide Thin Films

V. B. Sanap¹, A.V. Ingle²

^{1,2}Yeshwantrao Chavan College, Sillod, Dist. Aurangabad, (MS) India.

Abstract: Nanocrystalline cadmium sulfide (CdS) thin films have been prepared on glass substrate using a simple and inexpensive chemical deposition technique by varying the deposition parameters. The structural and morphological properties have been studied by x-ray diffractometer (XRD) and scanning electron microscopy (SEM). The optical and solid state properties such as absorbance/ transmittance/ reflectance, refractive index, extinction coefficient, dielectric constant, optical conductivity have been investigated for the photovoltaic applications. The band gap measured was found to be in the range 2.39 eV to 2.68 eV. The physical conditions were kept identical while growing all the samples.

Keywords: Cadmium sulfide, chemical deposition, thin films.

I. INTRODUCTION

Numerous techniques have been reported for the preparation of thin films such as spray pyrolysis, sputtering, electro deposition, vacuum evaporation, chemical vapour deposition technique. Out of this chemical deposition technique has become more popular in recent decades, especially for thin film deposition, due to its numerous advantages. It is easy, inexpensive and convenient method for large area preparation of thin films, at close to room temperature. Also films can be deposited on different kinds, shapes and sizes of substrates [1-4].

CdS is an important & useful material for optoelectronic applications, because its expected gap emission lies very close to the highest sensitivity of the human eye. Thus one might assume that CdS thin films are an appealing host for photonic devices. For the development of such optoelectronic devices, CdS thin films require comprehensive optical & solid state characterization. The physical properties were studied earlier by our group [10, 11].

In this work, effects of cadmium ion source on the optical & solid state properties of CdS thin films were reported. The objective is to provide the comprehensive study of optical & solid state properties of CdS thin films useful for optoelectronic applications, especially solar cells.

II. EXPERIMENTAL DETAILS

Thin films of CdS were deposited by the controlled chemical deposition technique using various cadmium ion sources as cadmium chloride, cadmium sulfate, cadmium nitrate and cadmium Iodide and thiourea as sulfur ion source. 0.1 M cadmium ion source solution and an equal volume of 0.2 M thiourea solution was added in 100-120 ml of de-ionized water. Ammonia was added slowly to adjust the pH. The solution was stirred and transferred to another container containing substrate. The resulting solution was kept at $70 \pm 2^\circ\text{C}$ for 40 minutes. The substrate used is glass slide. Cleaning of substrate is important in deposition of thin films. The crystallographic structure of films was analyzed with a diffractometer (EXPERT-PRO) by using Cu-K α lines ($\lambda = 1.542\text{\AA}$). The average grain size in the deposited films was obtained from a Debye-Scherrer's formula. Surface morphology was examined by JEOL model JSM-6400 scanning electron microscope (SEM). Optical properties were measured at room temperature by using Perkin-Elmer UV-VIS lambda-35 spectrometer in the wavelength range 100-1000nm.

III. RESULTS AND DISCUSSION

A. Effect Of Cadmium Sources On Film Thickness, Structural & Surface Morphology

Fig. 1 shows XRD pattern of CdS films for different cadmium sources. A comparison of the peak position (2θ values) of the JCPDS XRD spectra data for CdS suggests that the as-deposited CdS films have the cubic structure with the X-ray diffraction peaks corresponding to (111), (200) and (311) peaks. It was also observed that the diffraction angle (2θ) is different for different cadmium source used. The fourth peak (220) was detected in case of CdI₂ based films, which is also cubic in nature. The lattice parameter (a) have been calculated which is in agreement with the standard data (0.582nm). [Table 1]



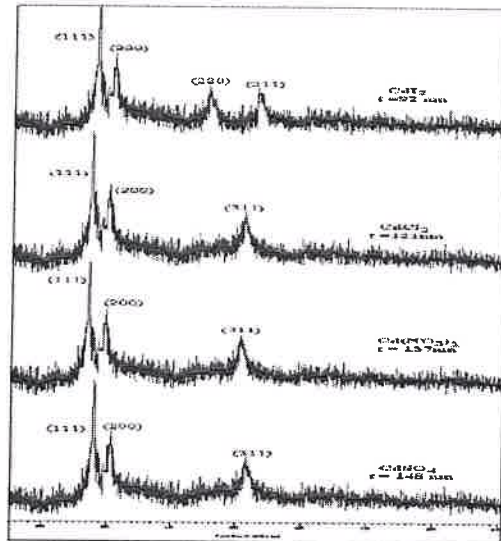


Fig.1. XRD pattern of CdS films for different cadmium sources

The average size of grain (g) has been obtained from the XRD patterns using Debye-Scherrer's formula, [8]

$$g = K\lambda / \beta \cos\theta \quad \dots(1)$$

Where, K = constant taken to be 0.94,

λ = wavelength of X-ray used (1.542Å),

β = FWHM of the peak and

θ = Bragg's angle.

Table 1 shows the grain size for different cadmium sources used. Highest grain size of CdSO₄-based films shows a much faster growth rate than other three films; this may due to cluster by cluster deposition process whereas in other cases smaller grain size may due to ion by ion deposition process. The SEM micrographs shows much smoother and more uniform films in case of CdCl₂ based films. The grain size obtained from SEM matches with the grain size obtained by XRD.

B. Optical Studies

Fig. 2 shows the optical absorbance spectra of cds thin films for all four cadmium sources. All the films shows low absorbance in the visible/near infrared region from ~500nm to 1100nm. However the absorbance is more than 80% in the ultraviolet region. It is observed that with the cadmium source the absorbance edge shifts towards the longer wavelengths. Similar behaviors in the optical spectra of cds films prepared by other technique have been reported elsewhere [5,6]. The sharp fall in absorbance near 500nm is an identification of good crystallinity of films. [8,9]

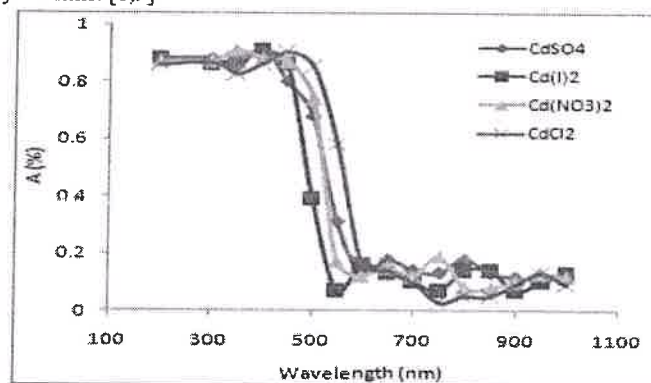


Fig. 2 Plot of $(\alpha h\nu)^2$ vs $h\nu$ for all cds films

From the absorbance data, the absorption co-efficient α was calculated using Lambert's law [10],

$$\ln(I_0/I_t) = 2.303 A = 2.303 \log 1/T = \alpha d \quad \dots(2)$$

Where, I_0 and I_t are the intensity of incident and transmitted light respectively. A - absorbance, T - optical transmission and d - film thickness.

The absorption co-efficient α was found to follow the relation, [7]

$$\alpha = [A (h\nu - E_g)^{1/2}] h\nu \quad \dots(3)$$

The band gap E_g was determined from each film by plotting $(\alpha h\nu)^2$ versus $h\nu$ and then extrapolating the straight line portion to the energy axis at $\alpha = 0$. The band gap energy E_g obtained for each Cd source is different. $CdCl_2$ -based film has the least band gap (2.39eV) and $CdSO_4$ -based film has highest band gap (2.68eV). The band gap of other two films is intermediate. Fig. 3 shows all band gap values observed are closest to the band gap of single crystal CdS (2.42eV) [7-9].

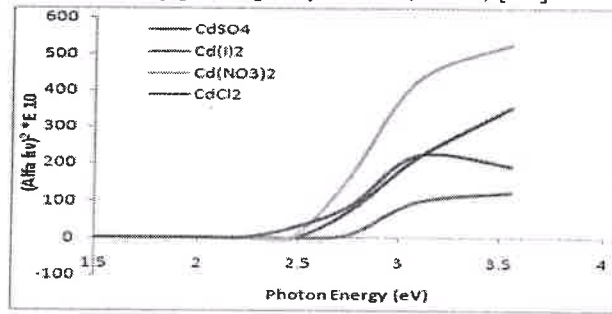


Fig. 3 Plot of $(\alpha h\nu)^2$ vs $h\nu$ for all CdS films

The variation of refractive index (n) with $h\nu$ for all CdS thin films is shown in fig 4. The average values of n ranged between 1.997 and 2.112 with maximum values that ranged between 2.196 and 2.474 as the Cd source changes from $CdSO_4$ to CdI_2 .

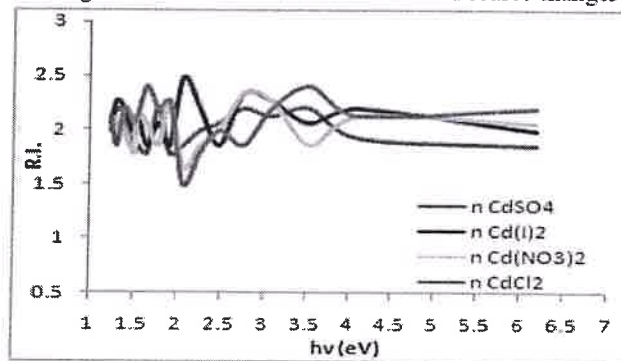


Fig. 4 Variation of R I (n) with wavelength for all CdS thin films.

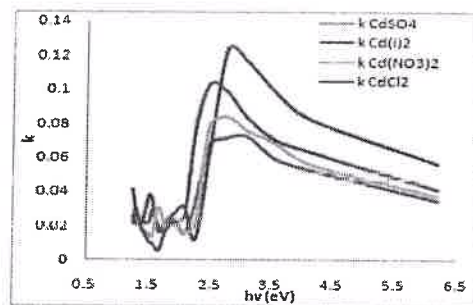


Fig. 5 Variation of k with $h\nu$ for all CdS thin films

The variation of extinction coefficient (k) with $h\nu$ for all CdS thin films is shown in fig 5. The average values of k ranged between 0.0367 and 0.0508 with maximum values that ranged between 0.0722 and 0.1233 as the Cd source changes from $CdSO_4$ to CdI_2 .

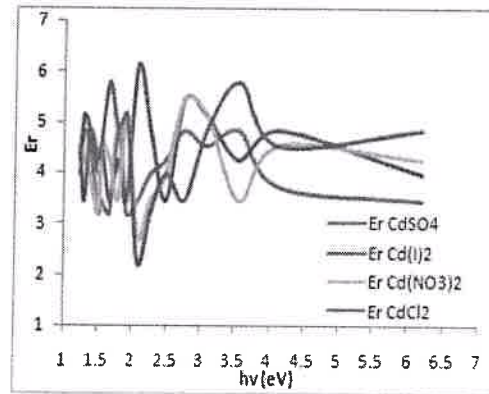


Fig. 6 Variation of ϵ_r with wavelength for all CdS thin films.

The plot of ϵ_r and ϵ_i against wavelength are shown in fig. 6 and Fig. 7 respectively. The average values of ϵ_r ranged between 3.92 and 4.47 with maximum values that ranged between 4.93 and 6.18 as the Cd source changes from CdSO₄ to CdI₂.

On other hand the average values of ϵ_i that ranged between 0.19 and 0.36 with maximum values that ranged between 0.67 and 1.39 as the Cd source changes from CdSO₄ to CdI₂ for all the samples.

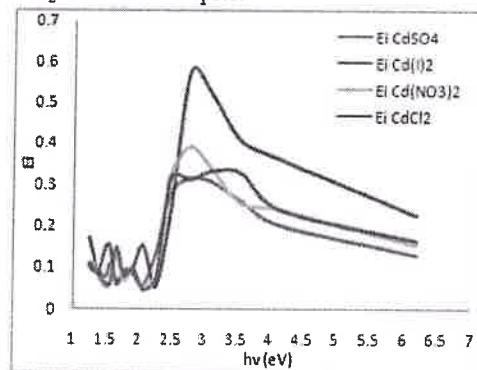


Fig. 7 Variation of ϵ_i with wavelength for all CdS thin films.

A plot of optical conductivity (σ) against wavelength is shown in Fig. 8. It has the average values that ranged between $3.056 \times 10^{13} \text{ S}^{-1}$ and $4.645 \times 10^{13} \text{ S}^{-1}$ with maximum values that ranged between $7.108 \times 10^{13} \text{ S}^{-1}$ and $12.143 \times 10^{13} \text{ S}^{-1}$ as the Cd source changes from CdSO₄ to CdI₂.

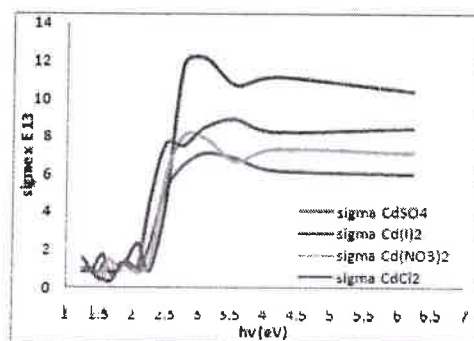


Fig. 8 Variation of σ with wavelength for all CdS thin films.

It is observed that the values of optical constants (n , k , ϵ_r , ϵ_i , σ) were very sensitive with the Cd ion source. The value of optical conductivity is high in case of CdI₂. Table 1 shows the optical and solid state properties with the Cd ion source and thickness of CdS thin films.



Table 1.

Optical & solid state properties with Cd sources for all CdS thin films.

Cd source	Grain size (nm)	Max n	Max k	Max ϵ_r	Max ϵ_i	Max $\sigma \times 10^{13} S^{-1}$	Energy bandgap (eV)
CdSO ₄	3.852	2.20	0.072	4.82	0.32	7.11	2.68
Cd(NO ₃) ₂	3.086	2.34	0.084	5.44	0.39	8.03	2.50
CdCl ₂	3.090	2.41	0.103	5.77	0.33	8.92	2.52
CdI ₂	2.911	2.48	0.123	6.12	0.58	12.14	2.39

IV. CONCLUSIONS

CdS thin films with various Cd ion sources have been successfully deposited by chemical deposition technique. The effects of Cd source on structural, morphological, optical and solid state properties have been studied. The XRD study reveals that the as-deposited CdS films are cubic structured with the average grain size between 2.9nm and 3.8nm. The UV-VIS spectroscopy showed high (>80%) transmittance, and low absorbance in the visible near infrared region from ~500nm onwards and poor transmittance in UV region. This makes the films suitable for optoelectronic devices, for instance window layers in solar cells also effective as protective coatings.

V. ACKNOWLEDGEMENTS

The authors are grateful to Head, DME, VNIT, Nagpur for providing XRD and SEM facilities. We would also like to acknowledge Head of Instrumentation Cell, SGBAMU for UV-VIS-Near IR facilities.

REFERENCES

- [1] Arturo Morales-Acevedo, Solar Energy, 80, 675, 2000.
- [2] Paulson P D & Dutta V, Thin Solid Films, 370, 299, 2000.
- [3] Emziane M, Durose K, Romeo N, Bosio A & Halliday D P, Thin Solid Films, 480, 377, 2005.
- [4] Panda S K, Chakrabarti S, Satpati B, Saryam P V & Choudhuri S, J Phys D Appl Phys, 37, 628, 2004.
- [5] Pawar S H, Bhosale C H, Bull. Matter Sci., 8 3, 419-422, 1986.
- [6] Sahay P P, Nath R K and Tiwari S, Cryst Res Technol, 42 3, 275-280, 2007.
- [7] Grecu R, Popovici E J, Ladar M et al, Journal of Optoelectronics & Advanced Materials, 6 1, 127-132, 2004.
- [8] Nair P K, M.T.S. Nair et al, J. Phys D, 22, 829, 1989.
- [9] Kitaev G, Mokrushin S, Urtskaya A, Kolloidn Z, 27, 51, 1965.
- [10] Sanap V B, Pawar B H, Chalcogenide Letters, 7, 3, 227-231, 2018.
- [11] Kawar S S, Sanap V B, B.H.Pawar, S.U.Hiswankar, Bionano Frontier (NSCTMS-2011), Dec 2011, 158-160.
- [12] Sanap V B, Pawar B H, Optoelectronics and Advanced Materials-Rapid comm. Vol. 5, No. 5, 530-533, 2011.
- [13] A.V.Feitosa, et al., Brazilian Journal of Physics, vol. 34, 2B, 2004.
- [14] Y.A. Salazar et al., Brazilian Journal of Physics, vol.36, No.3B, 2006.
- [15] J.G.Vazquez Luna et al., Cryst. Res. Technol. Vol.34, No. 8, 949-958, 1999.
- [16] I. Oladeji, I.Chow, J.Electrochem. Soc. 144, 2342, 1997.
- [17] M.Maleki, M. Sasani Ghamsari, sh Mirdamadi, R. Ghasemzadeh, Semi-conductor Physics-Quantum Electronics and Optoelectronics 10, 30, 2007.
- [18] T.Nakanishi, K. Ito, Sol. Energy Mater. Sol.Cells 35, 171, 1994.
- [19] A.Adachi, A.Kudo and T.Sakata, Bull.Chem. Soc.Jpn 68, 3283, 1995.




PRINCIPAL
Yeshwantrao Chavan College of
Arts, Commerce & Science, Sillod
Dist. Aurangabad.